

## Catalytic performance of CeAPSO-34 molecular sieve with various cerium content for methanol conversion to olefin

Mehdi Sedighi<sup>\*,†</sup>, Mostafa Ghasemi<sup>\*\*</sup>, and Alireza Jahangiri<sup>\*\*\*</sup>

<sup>\*</sup>Department of Chemical Engineering, University of Qom, Qom, Iran

<sup>\*\*</sup>Petroleum Engineering Department, Universiti Teknologi PETRONAS, Seri Iskandar, 32610, Perak, Malaysia

<sup>\*\*\*</sup>Faculty of Engineering, Shahrekord University, Shahrekord, Iran

(Received 14 June 2016 • accepted 21 December 2016)

**Abstract**—A series of CeAPSO-34s with various cerium contents was synthesized and characterized by multiple techniques such as XRD, SEM, BET, <sup>29</sup>Si MAS NMR, NH<sub>3</sub>-TPD and CO<sub>2</sub>-TPD. NH<sub>3</sub>-TPD spectra showed that a number of acid sites, especially those of strong acidity, is reduced with the increasing of Ce incorporation. Incorporation of metal ions gave rise to more silica-islands in the CeAPSO-34 framework. CO<sub>2</sub>-TPD showed that basic sites on the surface of modified samples are due to the presence of Ce-containing species incorporation into the framework of CeAPSO-34 molecular sieves. The performance of the catalysts was studied in methanol to olefin reactions at 425 °C under the atmospheric pressure. The results showed that the incorporation of cerium ions had great effects on the structure and acidity of the molecular sieves. All SAPO-34 and MeAPSO-34 molecular sieves were the very active and selective catalyst for light olefins production. Cerium incorporation improved the catalyst lifetime and favored the ethylene and propylene generation. However, an excess Ce content resulted in an inferior catalytic performance and stability. Therefore, there existed optimal cerium content for a specific SAPO-34.

Keywords: SAPO-34, Ce Incorporation, Light Olefin, Characterization, Lifetime

### INTRODUCTION

The world reserves of natural gas have caused continued interest in new approaches to main petrochemical chemicals such as ethylene and propylene, the most important organic materials in the petrochemical industry to produce numerous polymeric materials, fibers and rubbers. Methanol to olefin (MTO) process is one of the promising alternatives to the current process, i.e., steam cracking, which uses petroleum resources as the feedstock [1-4]. Due to the light olefin production from natural gas or coal via methanol in the MTO process, it has been regarded as an alternative process in recent years [3].

Different studies approved that small pore silicoaluminophosphate molecular sieve SAPO34 is a good catalyst for converting methanol to olefin. This could be ascribed to the mild acidity and effective pore openings of SAPO-34 to adsorb only straight chain molecules such as primary alcohols, linear paraffins, and olefins. Branched isomers, aromatics, and diffusion of larger molecules such as aromatics are largely restricted [5-7]. Nevertheless, this molecular sieve deactivates rapidly with time-on-stream, especially when the reaction is carried out at high space velocity. Metal incorporation as a convenient way to modify the catalytic behavior has been extensively investigated for the MTO reaction [8-10].

Many elements have been incorporated into the SAPO34 framework by isomorphous substitution to form MeAPSOs molecular

sieves (Me: Be, B, Mg, Ti, Mn, Fe, Co, Ni, etc.) [11-14]. The high selectivity and lifetime are attributed to framework distortion and acidity modification after the incorporation of metal ions. For example, Lu et al. [15] reported that the modification of SAPO-34 with lanthanum and yttrium causes higher selectivity to light olefin, lower methane formation, and longer lifetime than the parent SAPO-34 catalyst in the MTO process. These performances were ascribed to the incorporation of La<sup>+3</sup> and Y<sup>+3</sup> into the framework of SAPO-34. The modified catalysts showed higher selectivity to light olefins and longer lifetimes [13]. NiAPSO-34 catalyst showed the best performance, where high yield of ethylene and propylene was determined with 100% methanol conversion.

Obrzut et al. [8] found that the modification of SAPO-34 with K and Ce could remarkably reduce a rapid deactivation of the catalyst. Tian et al. [16] modified Ce- SAPO-34 catalysts with three methods, i.e., the liquid ion exchange with air calcination, impregnation with air calcination and impregnation with steam calcination methods. The results indicated that compared to the SAPO-34 catalyst, the catalyst prepared by the impregnation of Ce<sup>+3</sup> and steam calcination showed the best modification effect, prolonging the lifetime by 70 min and improving the ethylene selectivity by 10% (mol).

Rare earth (RE) elements are very influential components of the commercial catalysts for the process of catalytic cracking of hydrocarbon [17]. Our previous work [18] showed that the lifetime and selectivity increased with the incorporation of cerium and lanthanum ions in SAPO-34. Metal incorporation improved the catalyst lifetime and favored the ethylene and propylene product. Concerning the yield of light olefins at 425 °C and 1 bar, NiAPSO-34 favored

<sup>†</sup>To whom correspondence should be addressed.

E-mail: sedighi@qom.ac.ir

Copyright by The Korean Institute of Chemical Engineers.

ethylene production, and CeAPSO-34 and LaAPSO-34 were helpful for propylene production. Light olefins yield decreased with time on stream for all the samples, although this decrease rate is lower for MeAPSO-34 than for the parent SAPO-34. The catalyst lifetime increased in an order as follows: Ce->La->Co->Ni->Fe->SAPO-34. The rare earth modified catalysts exhibited lower methanation than parent SAPO-34 and transition metal modified catalysts.

Up to now a few reports explained the correlation between cerium incorporation amount into SAPO framework and catalytic property improvement. The clarification of the effects caused by metal incorporation and the corresponding change in catalytic performance merit a more detailed investigation.

In this study, to improve the catalytic performance of the SAPO-34 catalyst, Ce was selected as the promoter. A series of CeAPSO-34s was synthesized and variation in physicochemical characteristics and acidity upon incorporation of different amounts of Ce within the framework were compared. Furthermore, the influence of Ce loading on the catalytic performance and lifetime was studied.

## EXPERIMENTAL

### 1. Synthesis

The sources of Al, P and Si were aluminum isopropoxide (AIP, Merck), phosphoric acid (85 wt%  $H_3PO_4$ , Merck), and Silicic acid ( $SiO_2$ , Merck), respectively. Used templates were 20 wt% an aqueous solution of tetraethylammonium hydroxide (Merck) and morpholine (Merck). The gel molar composition was  $1 Al_2O_3$ :  $1 P_2O_5$ :  $0.4 SiO_2$ :  $0.9 Mor$ ,  $1.1 TEAOH$ ,  $x Ce_2O_3$ ,  $60 H_2O$  ( $x=0-0.1$ ).

The mixture was then placed in a 100 ml Teflon-lined stainless steel autoclave. The autoclave was placed in an oven at 463 K for 36 hours. The solid product was recovered, washed with distilled water and dried at 110 °C for ten hours. As-synthesized product was then calcined in air at 823 K for five hours. All the samples were pelletized, crushed and sieved through 20-40 mesh in size. The obtained samples with  $x=0, 0.025, 0.05, 0.075, 0.1$  were denoted as SAPO-34, CeAPSO-34 (0.025), CeAPSO-34 (0.05), CeAPSO-34 (0.075) and CeAPSO-34 (0.1).

### 2. Characterization

The structure type and crystallinity of all the samples were checked by X-ray diffraction (XRD) patterns on an X-ray diffractometer (Bruker D8) using CuK $\alpha$  radiation ( $\lambda=1.54 \text{ \AA}$ ). Chemical compositions in the crystal were analyzed by inductively coupled plasma (ICP-OES, Perkin-Elmer 3300DV instrument) after dissolving the samples in 1 N nitric acid solution. Crystal size and shape of catalysts were analyzed by scanning electron microscopy (SEM) using Philips XL30 microscopes, operating at 20 kV. The BET surface areas of calcined samples were determined from isotherm data of nitrogen adsorption-desorption using Micromeritics ASAP-2010 analyzer. Before these measurements, the template free samples were heated at 300 °C under vacuum for some hours. The  $NH_3$ -TPD experiment was performed with a Micromeritics Autowin 2910 chemical adsorption apparatus. 0.2 g calcined samples were pre-treated at 300 °C under continuous flow of  $30 \text{ ml min}^{-1}$  helium and subsequently cooled to the adsorption temperature of 100 °C. The

$NH_3$  desorption was measured from 100 °C to 700 °C at a constant heating rate of 10 °C/min in a He flow.  $^{29}Si$  MAS NMR spectra were recorded at room temperature with a 4 mm probe scanning at 10 kHz. The internal standard for chemical shifts was 2, 2-dimethyl-2-silapentane-5-sulfonate sodium salt (DDS).  $CO_2$ -TPD was used to probe the basicity of the modified samples in a procedure similar to  $NH_3$ -TPD. The  $CO_2$ -TPD experiments involved using a TG-DSC thermal analyzer assembly.

### 3. Activity Measurement

Experiments were carried out at 425 °C and 1 bar in a flow-type fixed bed stainless steel reactor [4]. The reactor consisted of a 45 cm long and 1.51 cm outer diameter. The depth of the catalyst bed in the reactor was 5 cm. The catalyst was pretreated by heating it to 550 °C in a nitrogen flow ( $30 \text{ mL min}^{-1}$ ). Methanol conversion to olefins was tested at 425 °C. During the reaction bidistilled water was used as a diluent and co-fed with methanol into the reactor with a concentration of 70 wt% in the feed. The catalyst charge and feed flow rate was set to obtain space-time,  $\tau=W/F_{MeOH}^0$  to  $13 \text{ g}_{cat}\cdot\text{hr}/\text{mol}$ . The reactor effluent was quenched by passing through a heat exchanger. The condensed liquid hydrocarbon products and any unconverted reactant were collected in separating flash drum attached to exchanger; then the gas phase passed through a series of condensers and was entered in a filter in the final stage. The hydrocarbon products were analyzed online using a Hewlett-Packard 5890 flame ionization detector (FID) gas chromatograph (GC) equipped with Agilent J&W GS-alumina column and Plot column.

## RESULTS AND DISCUSSION

### 1. Crystalline Structure, Morphology and Chemical Composition

The XRD patterns of the calcined SAPO-34 and CeAPSO-34 catalysts are shown in Fig. 1. The position and the intensity of the diffraction peaks of all the synthesized samples are similar to those reported in the literature [19]. Compared with SAPO-34, the peak intensities of Ce-modified catalysts decreased, indicating that the incorporation of cerium affected the crystalline of SAPO-34. In fact, there is not any extra diffraction peak in comparison with parent SAPO-34. This is because the amount of Ce loaded in the

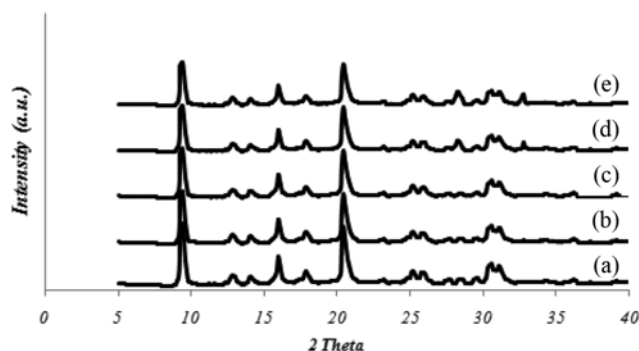


Fig. 1. XRD patterns of (a) SAPO-34, (b) CeAPSO-34 (0.025), (c) CeAPSO-34 (0.05), (d) CeAPSO-34 (0.075) and (e) CeAPSO-34 (0.1).

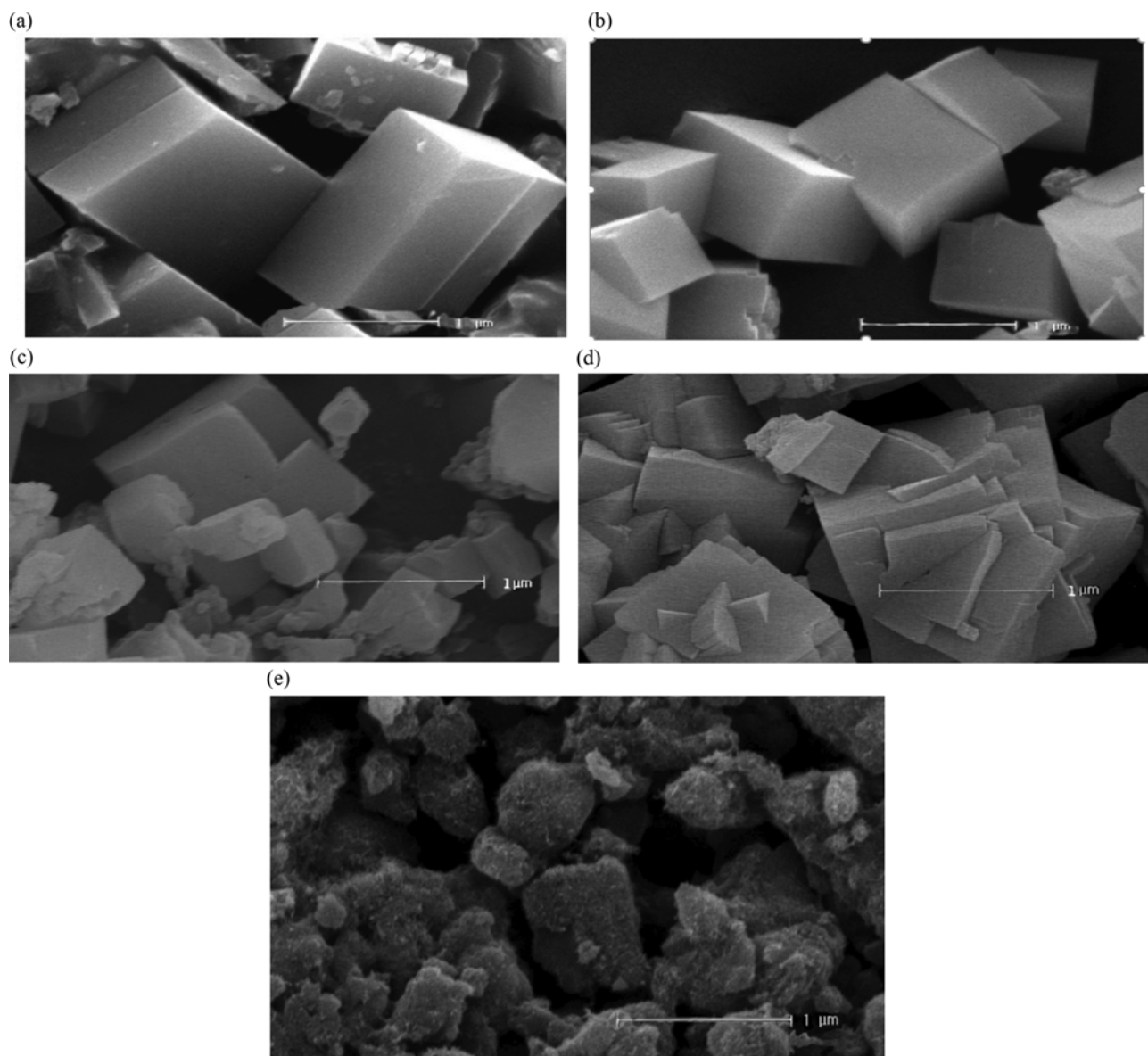


Fig. 2. SEM images of calcined samples of (a) SAPO-34, (b) CeAPSO-34 (0.025), (c) CeAPSO-34 (0.05), (d) CeAPSO-34 (0.075) and (e) CeAPSO-34 (0.1).

molecular sieve is very little, and in addition, Ce that dispersed evenly on the extra or inner surface of the zeolite was not loaded on the surface of the zeolite in this process.

All the synthesized CeAPSO-34 samples have a cubic morphol-

ogy, as shown in SEM images (Fig. 2), noting that the sizes of Ce-incorporated SAPO-34 crystals are a little smaller.

More kinks and steps are observed with Ce incorporation. These defects could reduce the crystallinity, which agrees with the XRD

Table 1. Physicochemical properties of CeAPSO-34 catalysts

Sample	Molar composition of crystals	Surface area (m <sup>2</sup> /g)			Pore volume (cm <sup>3</sup> /g)		
		S <sub>micro</sub>	S <sub>ext</sub>	S <sub>total</sub>	V <sub>micr</sub>	V <sub>meso</sub>	V <sub>total</sub>
SAPO-34	Al <sub>0.481</sub> Si <sub>0.112</sub> P <sub>0.407</sub> O <sub>2</sub>	572	18	590	0.29	0.08	0.37
CeAPSO-34(0.025)	Ce <sub>0.016</sub> Al <sub>0.467</sub> Si <sub>0.139</sub> P <sub>0.386</sub> O <sub>2</sub>	470	16	486	0.22	0.06	0.28
CeAPSO-34(0.05)	Ce <sub>0.019</sub> Al <sub>0.466</sub> Si <sub>0.133</sub> P <sub>0.382</sub> O <sub>2</sub>	452	14	466	0.19	0.04	0.23
CeAPSO-34(0.075)	Ce <sub>0.026</sub> Al <sub>0.458</sub> Si <sub>0.109</sub> P <sub>0.378</sub> O <sub>2</sub>	412	11	423	0.16	0.02	0.18
CeAPSO-34(0.1)	Ce <sub>0.042</sub> Al <sub>0.452</sub> Si <sub>0.095</sub> P <sub>0.375</sub> O <sub>2</sub>	395	12	407	0.12	0.02	0.14

data.

Table 1 depicts the chemical compositions and surface area of the calcined SAPO-34 and CeAPSO-34. Both the surface area and the micropore volume of the modified catalysts considerably decreased compared with the parent SAPO-34. It indicates that the metal ion dispersed into the channels of SAPO-34 in the modification procedures. The topology features narrow pores of 0.38 nm interconnecting multiple voluminous cavities to one another. The cavities have a maximum size of over 1 nm.

The composition of each catalyst, determined by ICP (ICP-OES, Perkin-Elmer 3300DV instrument), is given in Table 1. To compare the framework element substitution, initial gel composition of SAPO-34 and CeAPSO-34s had the same Al: P: Si ratio and identical templates. The chemical composition of the synthesized samples indicates that the presence of Ce in the starting gel affects the Si substitution into the molecular sieve frameworks. For samples with low content of Ce, upon incorporation of metals, more amount of Si was incorporated into the framework modified SAPO-34 catalysts and remained as amorphous silica on the extra-framework [20]. Increasing the Ce content for the sample CeAPSO-34 (0.075), and CeAPSO-34 (0.1), modification of cerium gave rise to an increase of the Si incorporation.

## 2. Chemical Environments, Acidity, and Basicity

$^{29}\text{Si}$  MAS NMR was performed to probe the Si environment into the SAPO-34 framework (Fig. 3). According to the literature [21], the peaks at  $\delta = -92.5, -96.5, -101, -106, -111$  are attributed to Si(4Al), Si(3Al), Si(2Al), Si(1Al), and Si(0Al) environments, respectively. Compared with SAPO-34, no additional peak is observed in the spectra of CeAPSO-34, indicating that no new Si species are generated with cerium incorporation.

The signals for coordination states of Si(4Al) and Si(3Al) show relatively high intensity while the signals for Si(2Al), Si(1Al) and Si(0Al) present comparatively low intensity. The band centered at  $-92.5$  ppm (Si(4Al)) represents that the Si atoms are in phosphorus position, and therefore, the silicon substitution is occurring only via the mechanism SM2 (a phosphorus atom substituted by a

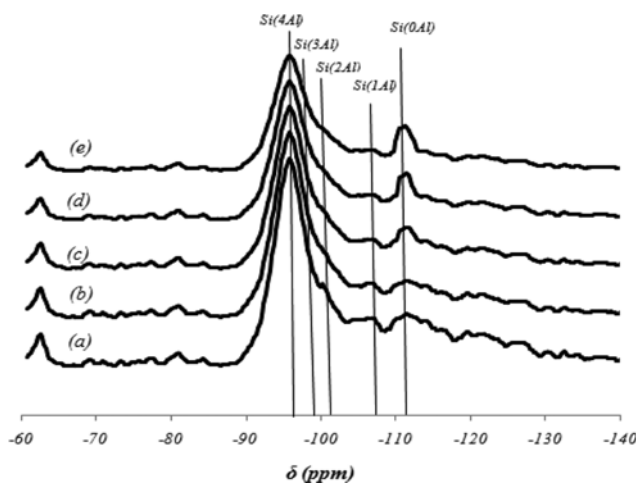


Fig. 3.  $^{29}\text{Si}$  MAS NMR spectra of samples, (a) CeAPSO-34 (0), (b) CeAPSO-34 (0.025), (c) CeAPSO-34 (0.05), (d) CeAPSO-34 (0.075) and (e) CeAPSO-34 (0.1).

silicon atom). This band is attributed to hydroxyl groups of the Brönsted acid sites. The other peaks occur if the silicon is incorporated into the framework via the substitution mechanism SM3, in which Si incorporates via a simultaneous substitution of a pair of adjacent Al and P atoms by two Si atoms [21,22]. A higher number of acid sites are generated through the SM2 mechanism.

The maximum amount of Si(4Al) species is shown for the non-modified sample, while the amount of Si(0Al) species became more substantial in the framework of Ce-incorporated samples, indicating more silica-islands formed in the CeAPSO-34 framework. Because of the prohibition of the Si-O-P bonding in the framework, the corresponding Si-O-Al region will be generated at the border of the Si island [10,23]. Strong acid sites will form in this Si-Al region, with the properties similar to silicoaluminated zeolite. These remarks agree well with the  $\text{NH}_3$ -TPD results.

The acidity properties of the samples were measured by temperature programmed desorption of ammonia (Fig. 4).

The profiles showed two peaks at 180–210 and 440–460 °C. These low and high desorption peaks match to the weak (P-OH hydroxyl groups not fully linked to  $\text{AlO}_4$  tetrahedra) and strong acid sites (Si-OH-Al hydroxyl groups), respectively. Table 2 lists the  $\text{NH}_3$ -TPD data of SAPO-34 and CeAPSO-34 catalysts. As expected, the catalyst acidity decreased after Ce adjustment and the total acidity

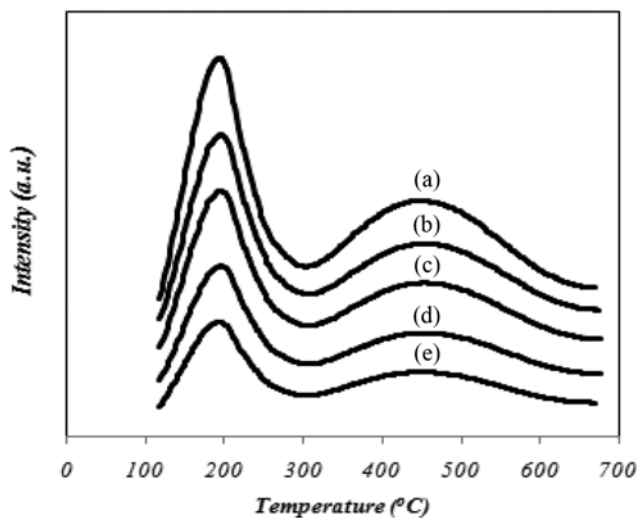


Fig. 4. TPD profiles of ammonia desorption of samples, (a) CeAPSO-34 (0), (b) CeAPSO-34 (0.025), (c) CeAPSO-34 (0.05), (d) CeAPSO-34 (0.075) and (e) CeAPSO-34 (0.1).

Table 2. Acidity measurement of samples with  $\text{NH}_3$ -TPD

Catalyst	Acidity <sup>a</sup>			
	Total	Weak	Strong	Strong/Weak
SAPO-34	1.0375	0.4350	0.6025	1.38
CeAPSO-34(0.025)	0.7362	0.3512	0.3850	1.09
CeAPSO-34 (0.05)	0.4474	0.2216	0.2258	1.02
CeAPSO-34 (0.075)	0.2575	0.1389	0.1186	0.85
CeAPSO-34 (0.1)	0.2360	0.1285	0.1075	0.83

<sup>a</sup>As mmol $\text{NH}_3$ /g; Weak from 180–220; strong from 430–480

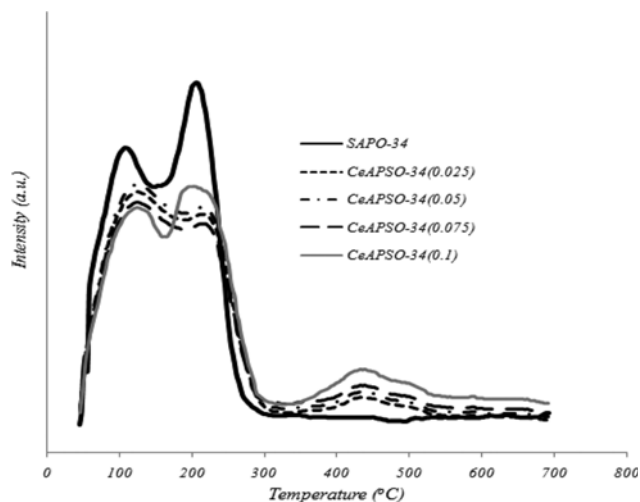


Fig. 5. The CO<sub>2</sub>-TPD plots of the calcined catalysts.

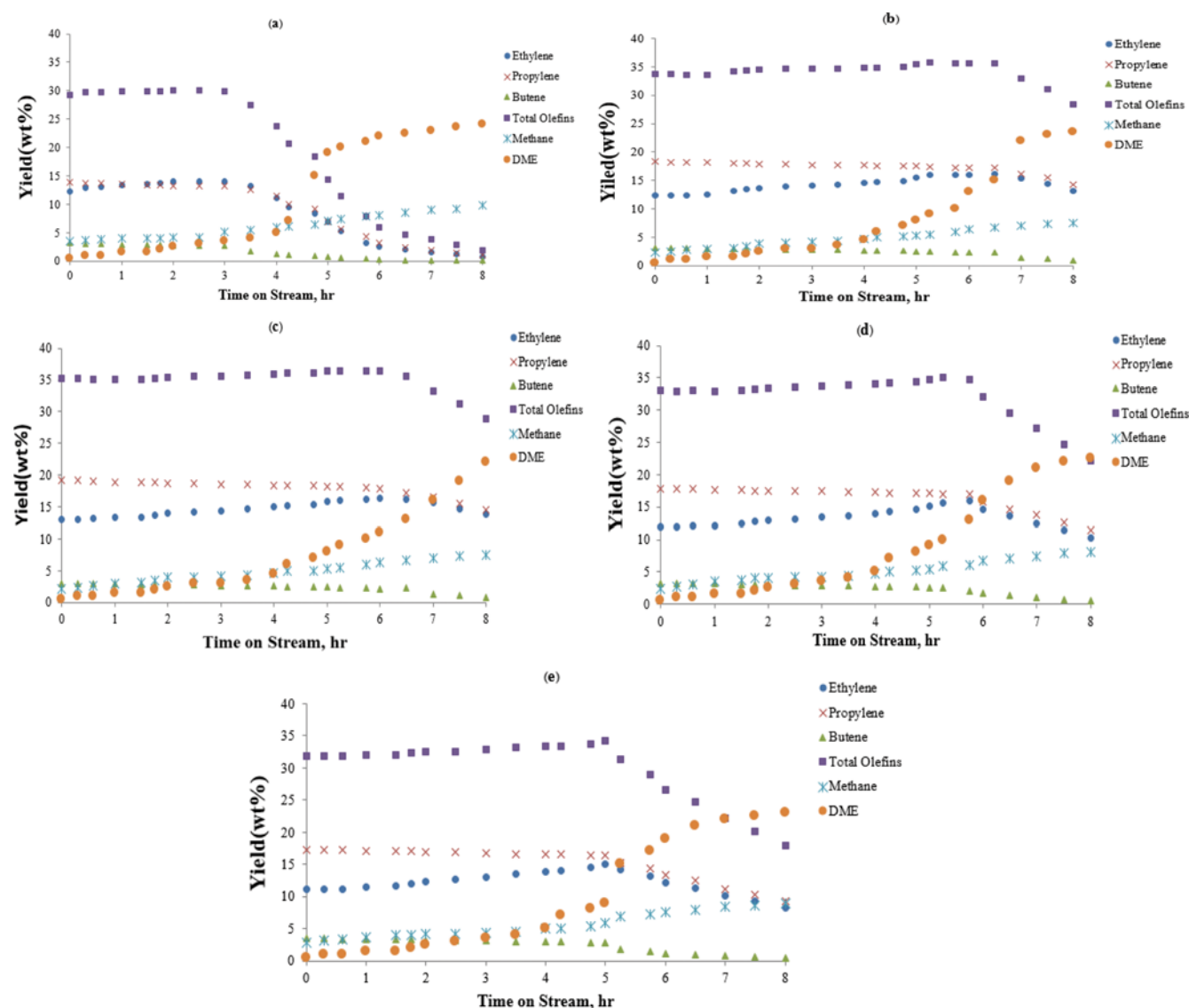


Fig. 6. Yields of light olefins over, (a) CeAPSO-34 (0), (b) CeAPSO-34 (0.025), (c) CeAPSO-34 (0.05), (d) CeAPSO-34 (0.075) and (e) CeAPSO-34 (0.1).

lessened with the increase of Ce loading. With the increment of Ce loading, both weak and strong acid sites decreased. When Ce content changed from 0.075 to 0.1, only a slight decrease of the total acidity was obtained. This may stem from less Si incorporation and the formation of more silica-islands in CeAPSO-34 samples with relatively high Ce content. Note that the strong acid sites decreased much faster than the weak acid sites, thereby the strong/weak ratio decreased with the increase of Ce loading.

The surface basicity of modified SAPO-34 with different Ce contents was measured by CO<sub>2</sub>-TPD. Fig. 5 indicates one more desorption curve was discovered at around 440 °C for modified samples, which can be thought to result from the strong interaction between CO<sub>2</sub> and basic sites. This modification can provide the basic sites needed for the transformation of methanol according to oxonium ylide mechanism [24-26]. With increasing Ce content to 0.1, the intensity of peak appearing at the high temperature increased. This peak represents the stronger basicity than the other two peaks.

### 3. Catalyst Testing

Catalytic conversion of methanol to light olefins was at 425 °C and space-time of over SAPO-34 and CeAPSO-34s. The evolutions of product yields as a function of M are given in Fig. 6. M is defined as the total weight of methanol fed to the reactor during the run per unit weight of catalyst. At initial times, light alkenes, such as ethylene, propylene and butenes, are the main products (more than 80% in total), indicating that SAPO-34 and modified catalysts are very selective catalysts for the production of light alkenes from methanol. The yield of ethylene increased gradually with process time, meanwhile, the yield of propylene and butene shows slightly decreases during the reaction. This is ascribed to the positive effect of coke accumulation on the ethylene formation that could suppress the formation of larger intermediates, which are the precursors of higher olefins, thus enhancing ethylene selectivity. The total light olefins reached a maximum at specified M for each catalyst; thereafter light olefin yield in the product decreased systematically. For all catalysts, deactivation is observed by a decline in olefin production and subsequent total light olefins breakthrough.

All samples gradually lost their activity by prolonged process time. The run time for methanol conversion increased with the increment of Ce content from 0 to 0.05, but decreased at 0.075 and 0.1 Ce content. This demonstrates that Ce incorporation into a SAPO-34 framework can enhance the catalytic activity of CeAPSO-34 catalysts. This could be attributed to the acidity adjustment by Ce incorporation.

MTO reaction is an acid-catalyzed reaction. However, this reaction can lead to the formation of byproducts such as higher olefin, aromatic, paraffin, and naphthenes [27,28]. The formation of these byproducts decreases the light olefin yield. A comparison between NH<sub>3</sub>-TPD data and catalytic operations shows that the decreased secondary reaction of light olefins could be related to the decrease of the catalyst acidity, especially strong acid sites. Acidity affects the secondary reactions. High densities of Brønsted acid sites, especially the acid sites in the neighborhood, are very important for hydrogen transfer reactions, oligomerization, and cracking. The latter reactions are responsible for coke deposition and thereby the deactivation of catalysts. The formation of the catalytic activity centers may be the reason for the increased light olefin yield due to Ce incorporation. Furthermore, the CeAPSO-34s greatly increased the lifetime of catalysts.

Fig. 6 indicates that the light olefin yields and lifetime increased with increasing Ce content to 0.05, but decreased at 0.075 and 0.1 contents. The acidity of the latter samples is lower than the CeAPSO-34 (0.05). This suggests that there exists another factor affecting the catalytic performance and can be justified by CO<sub>2</sub>-TPD data. Samples CeAPSO-34 (0.075) and CeAPSO-34 (0.1) represent high basicity at a higher temperature than the other modified samples. This relates to the excessive stronger basic sites. If the basic site is too strong, the molecule adsorbed on the basic site cannot be readily dissociated. Thus, the next step of the reaction cannot efficiently proceed.

### CONCLUSION

Cerium-incorporated SAPO-34 with a CHA zeolite structure

was synthesized for application in MTO process. The results indicated that the incorporation of metal ion had great effects on the structure and acidity of the molecular sieves. The results showed that Ce modification of the SAPO-34 increased both the MTO catalytic stability and the light olefin yield. However, there exists an optimal Ce amount for a specific SAPO-34. The sample CeAPSO-34 (0.05) had the best catalytic stability as well as the highest light olefin yield. The NH<sub>3</sub>-TPD spectra demonstrated that the incorporation of cerium brings about lower acidity. This could explain the catalytic stability improvement of MeASPO-34 compared to parent SAPO-34. Furthermore, the CO<sub>2</sub>-TPD characterization of the modified samples demonstrated that basic sites needed for MTO were provided by Ce incorporation.

### REFERENCES

1. M. Sedighi, M. Ghasemi, M. Mohammadi and S.H. A. Hassan, *RSC Adv.*, **4**, 28390 (2014).
2. T.-Y. Park and G. F. Froment, *Ind. Eng. Chem. Res.*, **43**, 682 (2004).
3. M. Sedighi, K. Keyvanloo and J. Towfighi, *Ind. Eng. Chem. Res.*, **50**, 1536 (2011).
4. M. Sedighi and J. Towfighi, *Fuel*, **153**, 382 (2015).
5. T. R. Cannan, E. M. Flanigen, R. T. Gajek, B. M. Lok, C. A. Messina and R. L. Patton, Google Patents (1984).
6. T. Yu, J. Wang, M. Shen and W. Li, *Catal. Sci. Technol.*, **3**, 3234 (2013).
7. Y. Iwase, K. Motokura, T. Koyama, A. Miyaji and T. Baba, *Phys. Chem. Chem. Phys.*, **11**, 9268 (2009).
8. Z. Li, J. M. Triguero, P. Concepción, J. Yu and A. Corma, *Phys. Chem. Chem. Phys.*, **15**, 14670 (2013).
9. B. Valle, A. Alonso, A. Atutxa, A. Gayubo and J. Bilbao, *Catal. Today*, **106**, 118 (2005).
10. Y. Wei, Y. He, D. Zhang, L. Xu, S. Meng, Z. Liu and B.-L. Su, *Micropor. Mesopor. Mater.*, **90**, 188 (2006).
11. M. Hartmann and L. Kevan, *Res. Chem. Intermediates*, **28**, 625 (2002).
12. T. Inui and M. Kang, *Appl. Catal. A: Gen.*, **164**, 211 (1997).
13. H.-N. Sun and S. N. Vaughn, Google Patents (1999).
14. B. M. Weckhuysen, A. A. Verberckmoes, M. G. Uytterhoeven, F. E. Mabbs, D. Collison, E. de Boer and R. A. Schoonheydt, *J. Phys. Chem. B*, **104**, 37 (2000).
15. J. Lu, X. Wang and H. Li, *Reaction Kinetics Catal. Lett.*, **97**, 255 (2009).
16. S. Tian, S. Ji, D. Lü, B. Bai and Q. Sun, *J. Energy Chem.*, **22**, 605 (2013).
17. W. Xiaoning, Z. Zhen, X. Chunming, D. Aijun, Z. Li and J. Guiyuan, *J. Rare Earths*, **25**, 321 (2007).
18. M. Sedighi, M. Ghasemi, M. Sadeqzadeh and M. Hadi, *Powder Technol.*, **291**, 131 (2016).
19. B. M. Lok, C. A. Messina, R. L. Patton, R. T. Gajek, T. R. Cannan and E. M. Flanigen, *J. Am. Chem. Soc.*, **106**, 6092 (1984).
20. M. Salmasi, S. Fatemi and A. Taheri Najafabadi, *J. Ind. Eng. Chem.*, **17**, 755 (2011).
21. T. Álvaro-Muñoz, C. Márquez-Álvarez and E. Sastre, *Catal. Today*, **179**, 27 (2012).
22. M. Sedighi, J. Towfighi and A. Mohamadalizadeh, *Powder Tech-*

- mol.*, **259**, 81 (2014).
23. G. Sastre, D. W. Lewis and C. R. A. Catlow, *J. Phys. Chem. B*, **101**, 5249 (1997).
24. M. A. Zanjanchi, A. Ghanadzadeh and F. Khadem-Nahvi, *J. Inclusion Phenom. Mol. Recognit. Chem.*, **42**, 295 (2002).
25. G. J. Hutchings and R. Hunter, *Catal. Today*, **6**, 279 (1990).
26. M. Sedighi, H. Bahrami and J. Towfighi, *J. Ind. Eng. Chem.*, **20**, 3108 (2014).
27. A. T. Aguayo, A. G. Gayubo, R. Vivanco, M. Olazar and J. Bilbao, *Appl. Catal. A: Gen.*, **283**, 197 (2005).
28. M. Stöcker, *Micropor. Mesopor. Mater.*, **29**, 3 (1999).